Scientific Research Publishing

Investigating the Damaging Effects of the Cyclic Discharge in the Uni-Axial Compression of *Raphia vinifera* L. Arecacea

Brice Poumegne Kouam[1,2]*, Didier Fokwa[3,4], Dieunedort Ndapeu[1,2,4], Médard Fogue[1,2]

[1]Research Unit of Mechanics and Physical Systems Modeling of (UR2MSP), Department of Physics, Faculty of Science, University of Dschang, Dschang, Cameroon
[2]Research Unit of Engineering of Industrial Systems and Environment (URISIE) IUT/FV Bandjoun, Department of Physics, Faculty of Science, University of Dschang, Dschang, Cameroon
[3]Laboratory of Mechanics (LM), Department of Civil Engineering, Advanced Teacher's Training College for Technical Education, University of Douala, Douala, Cameroon
[4]Laboratory of Mechanics and Appropriate Materials (LAMMA), Department of Civil Engineering, Advanced Teacher's Training College for Technical Education, University of Douala, Douala, Cameroon
Email: *brice.kouam@univ-dschang.org, *debriceko@gmail.com

Abstract

The bamboo stem, when mature 5 to 6 years, serves as a building material for modest houses and its marrow as packaging purposes. One of the strains related to the uses of bamboo stem is most often the compression towards the axial direction. The phenomenon of damage is very often observed during such loading. The present study on raffia aims to analyze this phenomenon through cyclical stresses as usual. From the results obtained, it was observed in the stress-strain plane, that the area of the hysteresis loops and the residual strain evolve with two parameters: the number of cycles and the stress peaks. The study of energy dissipation has shown that it evolves according to an exponential law as a function of the number of cycles. The distribution of the energy rate along a stem shows that the samples from the zone close to the base store twice (0.0412 MJ/m^3) more energy than the samples taken from the top of the foliage (0.019 MJ/m^3).

Keywords

Bamboo, Raphia, Cyclic Compression, Energy Dissipation

1. Introduction

The forest kingdom is made up of many species of plants, whose potential is enormous in the economic and ecological terms for certain population on the sur-

face of globe. The term bamboo is attributed to most tallgrass. According to publisher INBAR [1], the different types of bamboo are between 60 and 90 for more than 1100 species mainly distributed in the tropical and equatorial zones of Africa and America. The species studied in this paper belong to the raffia genus and monocotyledon class of trees called *vinifera* [2]. Its structure from the inner to the outer part is made up of a very hard outer thin layer call a shell. It contains a spongy central part called the cork which responsible for the great bamboo flexibility [3].

It is an eco-material with diverse assets. It is used for construction projects and develops a healthy atmosphere in buildings. Foadieng [4] research work has shown that it has excellent thermal properties. In addition to his good thermal properties, other research based on analysis and mechanical characterization ([2] [5] [6]) has revealed that bamboo has remarkable mechanical properties.

The cyclic charging technic has been widely used by many researchers and on various materials. A good number of works ([7] [8] [9]) for example were carried out to understand the behavior under the cyclic charge of reinforced concrete or not. Concerning the bamboo species *Oxytenantera abyssinica and Bambusa vulgaris*, the work of Fozao *et al.* [10] carried out on these species has shown that the degradation phenomena generated during cyclic loading in the plastic domain can be modeled by endochronic theory. In addition, Pambou Nziengui *et al.* [11] carried out cyclic compression tests on wood called okoumé. Results reveal that this material loses more than 30% of its resistance capacity under cyclic loading; which is moreover in agreement with Euro-code 5 which postulates that under a cyclic loading, the assemblies lose nearly 30% of their mechanical resistance. The *Pericopsi elata* species was studied under cyclic loading [12]. This study shows that while the damage evolves from one cycle to another, the Young's modulus also decreases; a sign that the material is damaged. In addition, he observes that the critical threshold of the damage variable is lower than the theoretical value of damage in the 03 directions under loading. This information will be confirmed the same year by the research of Fothe *et al.* [13] during the study of the behavior under cyclic loading of the species *Entandrophragma cylindricum* (sapelli) and *Chlorophora exelcia* (iroko).

However, despite a good number of works mentioned above, no research work on the study under cyclic loading in the uni-axial compression of the raffia bamboo has not yet to our knowledge been a subject of a paper. The purpose of this paper is to provide an answer to understanding the behavior of bamboo when it is subjected to loading-unloading cycles in compression. These results could make it possible to consider and optimal use of the raffia bamboo in the structural field of construction. In Cameroon and precisely in the north and southwest areas, the buildings are made thanks to the experiences drawn from here and there.

2. Materials and Methods

2.1 Materials

2.1.1. Plant Material

The raffia stems on which the study will focus are taken in Cameroon from the

marshy lowlands. A raffia palm is usually made up of four parts. The spine, the seed, the leaflet and the petiole [3]. The latter is our object of study. The selected pétioles therefore show no macroscopic observable defect. The dimensions vary depending on the diameter between 32 and 37 mm and in the length between 5 m and 8 m.

2.1.2. Sampling

The stem is cut into for codified parts ranging from 1/4 linked at the base to 4/4 linked at the top. This codification is in agreement with the work of Sikame *et al.* [2]. The idea is to assess the mechanical behavior of the specimens following different sampling zones. The test specimens are taken from different parts using sharp cutting tool (**Figure 1**).

2.2. Characterization Method

2.2.1. Water Content

Humidity is an important physical parameter to consider prior to any feasible biomaterial test. Our samples were conditioned according to a well-defined protocol [14]. According to standard ISO 2004, a constant mass is considered when the results of two successive weighing carried out at a time of 6 hours do not vary by 0.1% of the mass of the test specimen. The selected samples are conditioned at a temperature of 60°C. The moisture content is defined as the ratio between the difference of the initial mass and the anhydrous mass by the anhydrous mass. The relative humidity of the weighed samples is 12.6.

$$H = \frac{\left(M_H - M_0\right)}{M_0} \times 100 \tag{1}$$

where H is the water content;

M_H the mass sample with water content;

M_0 is the anhydrous mass;
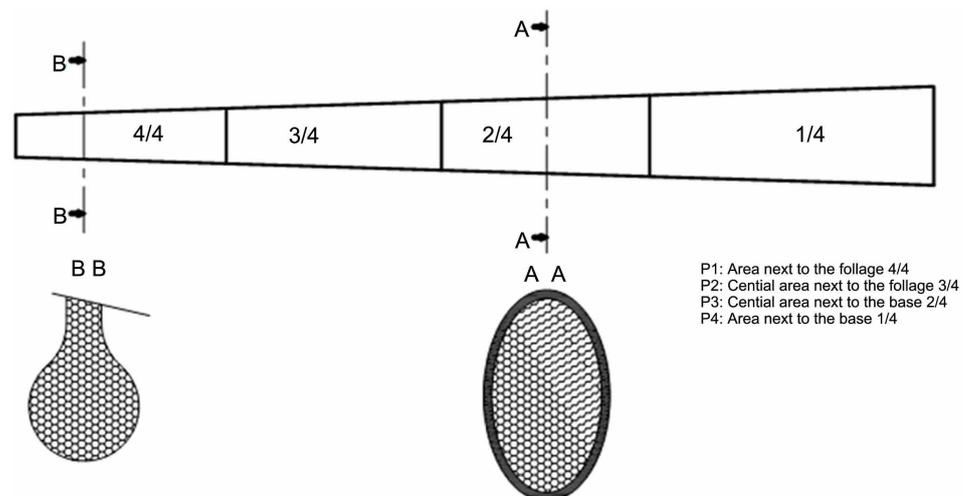
$(M_H - M_0)$ the mass water contained in the specimen.

Figure 1. Sampling area.

2.2.2. Data Acquisition Equipment

Once harvested from the fields, the stems are brought back to the laboratory. An Ecolog brand thermo-hygrometer use to read the ambient temperature of the laboratory and to make sure that the tests carried out are at the temperature recommended by standard norm [14]. The electronic balance of precision 1/100th was used for weighing samples. The compression test was carried out on an INSTRON 1/100th precision digital acquisition device. All these data are entered into personal computer with Excell 2013 and MATLAB 2014 software for the programming of curves all samples are tested at a relative humidity of 12.6 (**Figure 2**).

2.2.3. Charging and Discharging Method in Uni-Axial Compression

In this section, the test samples are carefully selected taking into account their dimensions (diameter and lenght) in accordance with standard norm [14]. The average diameter is 33 mm and the height 40 mm for the chosen samples. The lack of parallelism between the upper and lower faces of the samples in 0.01%. The tests are carried out on the INSTRON machine with a loading speed calibrated at 0.4 mm. The piloting under stress is the changing method use. The level of applied uni-axial constrain increases according to a average strain of 2.50 MPa. The increment in stress is piloting to the range 0 à 4.35; 0 à 3.84; …; finally from 0 to 14.81 MPa as in **Figure 3**. This methodology is repeated several times on four samples from the differents sampling zones. The test curves obtained on specimens from the same zone are fairly reproducible. Thus, the following analysis will be based on the curve of the sample taken from zone 2/4.

3. Results and Discussion

3.1. Hysteresis Loops and Characterization of Energy Release Rate

Figure 4 shows that the charge and discharge curves do not coincide. This leads to the formation of hysteresis loops. Indeed, during the loading phase, the fibers deform according to a plastic behavior. The material stores energy during this phase. During unloading, the fibers under stress gradually relax, a sign of restitution of the energy previously stored. The energy evaluated for a loop thus corresponds to the difference between the energy stored and that released. Thereafter, the area of hysteresis loops increases with the number of cycles.
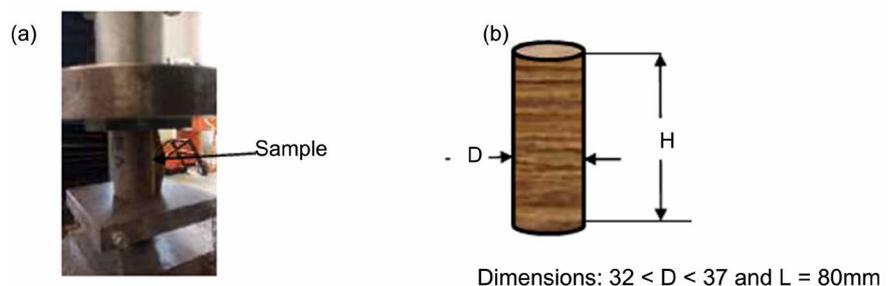

Figure 2. Image of test sample on compression (a) and dimensions of sample (b).
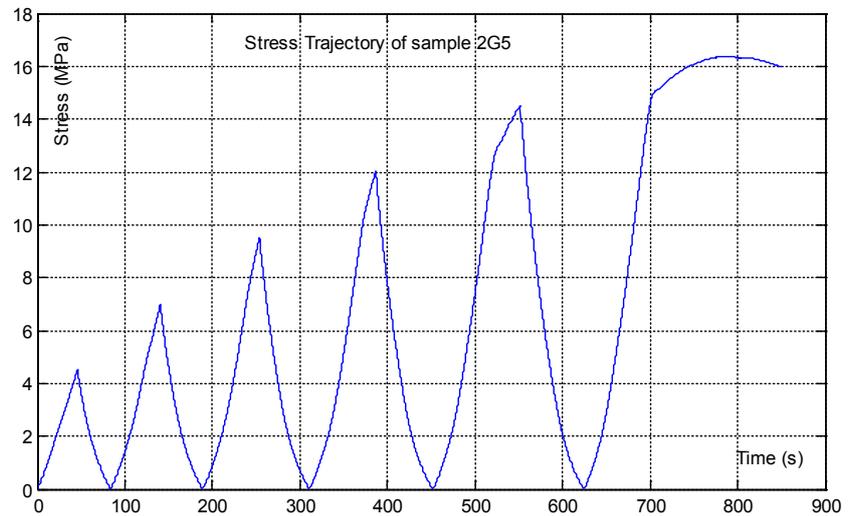
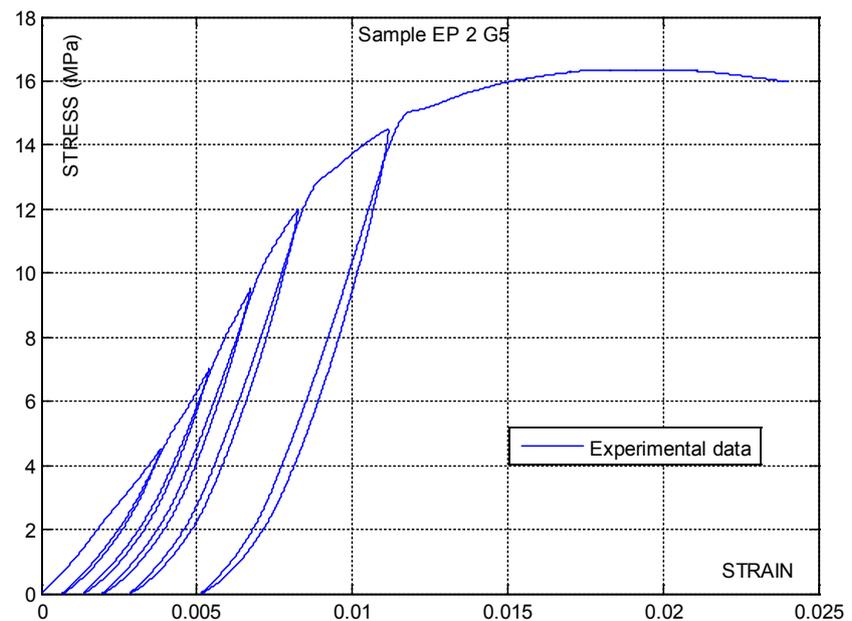**Figure 3.** Stress trajectory following charge-discharge.

Figure 4. stress-strain curve of a cyclic compression test.

In order to evaluate the rate of energy restored for a cycle, we used the following relation:

$$\Delta U_i = \int_{\varepsilon_{r1}}^{\varepsilon_{r2}} \sigma_i \mathrm{d}\varepsilon_i - \int_{\varepsilon_{u2}}^{\varepsilon_{u1}} \sigma_i \mathrm{d}\varepsilon_i \tag{2}$$

where ΔU_i is the energy store in the ième cycle consider. ε_{r1} et ε_{r2} are respectively the deformation at the beginning and end of the discharge. ε_{u2} et ε_{u1} are respectively the deformation at the beginning and end of the charge. σ_i is the maximum stress corresponding to the hysteresis loop.

Since the charge and discharge cycles corresponding to the release of energy from hysteresis loops, the total energy restored corresponds to the critical step

which supposes complete material rupture is equal to the sum of energy release by each cycle. It is given by relation (3).

$$\Delta U = \sum_{i=1}^{n} \Delta U_i \tag{3}$$

Figure 5 illustrates perfectly the use of relation (2).

Table 1 shows the energy variation along a stem.

In view of a statistical data in Table 1, it appears the energy rate captured by the hysteresis loop changes when the number of cycles increases. Figure 4 shows the energy variation rate by the sampling area. On the other hand, Figure 7 shows the linear energy evolution with the stress level for each hysteresis loop concerning EP 2/4 G5 sample.

Figure 6 shows that the energy stored decreases when we move from the area near to the base to the area near the foliage. In addition, a sample drown from an area close to the base absorbs twice as much energy as that taken from top of the top of the stem (Figure 6).

The relationship between the energy stored and the number of cycle per sampling area is given in Figure 8(a). In Figure 8(b), it is clear that the low of evolution which governs the cumulative energy as a function of the number of cycles is an exponential form.

Table 1. Energy transfer by hysteresis loops at each cycle (MJ/m^3).

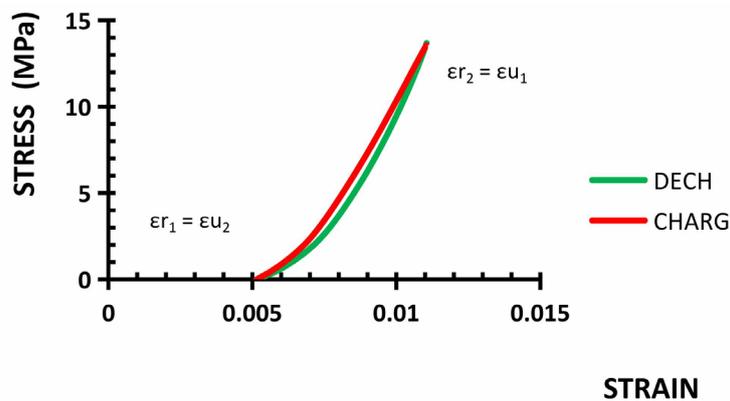| Number of cycle	Zone 1/4	Average	Zone 2/4	Average	Zone 3/4	Average	Zone 4/4	Average
1	0.0125		0.0128		0.0125		0.0085	
2	0.0221		0.0205		0.0191		0.0169	
3	0.0295	**0.0412**	0.0275	**0.028**	0.0326	**0.026**	0.0233	**0.019**
4	0.0396		0.0327		0.0314		0.0295	
5	0.0429		0.0465		0.0363		-	
6	0.0491		-		-			
7	0.0930		-		-			

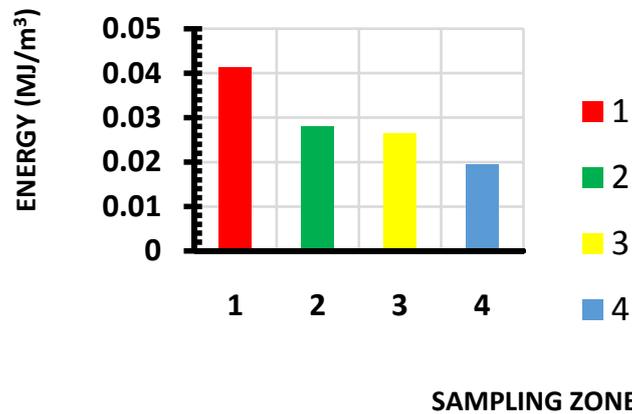Figure 5. Typical curve stress-strain for the 5th cycle.

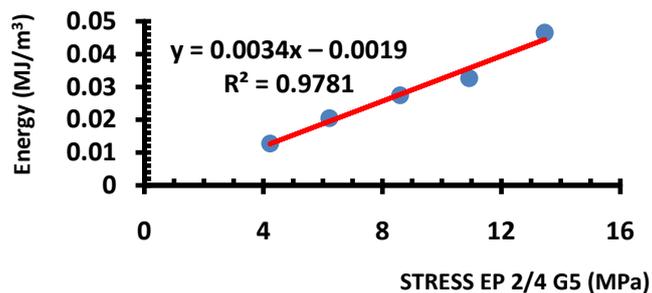**Figure 6.** Variation of energy rate by sampling area.

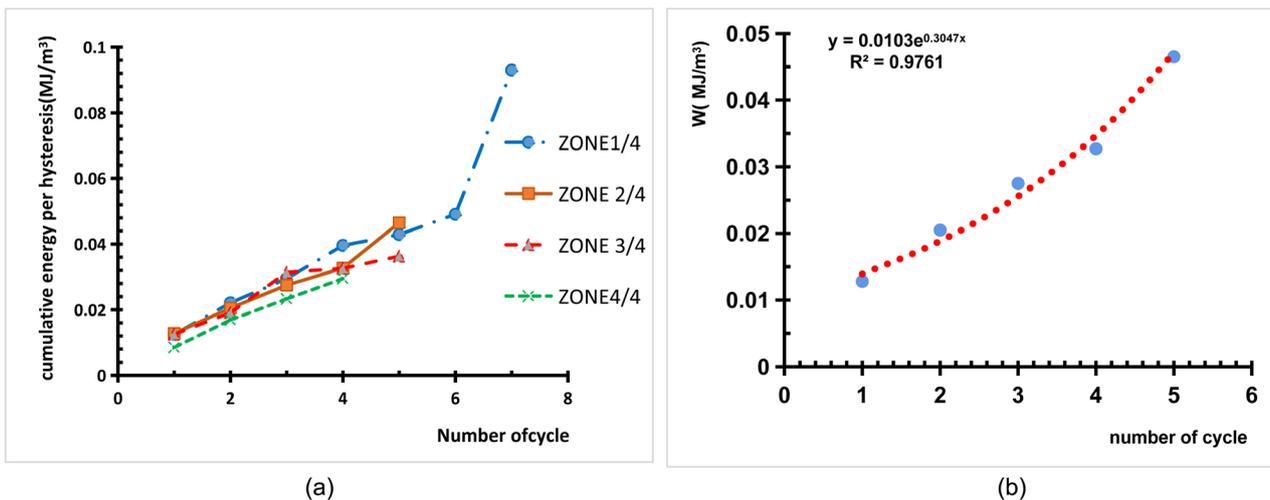**Figure 7.** Energy curve as function of the strain level per cycle.

Figure 8. cumulative energy curves by hysteresis as a function of the number of cycles.

3.2. Analysis of the Rigidity of the State of Damage with Respect to the Number of Cycle

The curves of the stress strain deformation from the other zones and similar to that of **Figure 4** made it possible to collect the data on the Young modulus of the slopes of charge and discharge. **Figure 9** presents a set of curves contained in the stress-number of cycles plane. In general, it is observed that the evolution of the loading range is accompanied by an increase in the number of cycles. However,

Table 2. Young's modulus of charge and discharge slopes (MPa).

Cycles Charge (C)-Décharge (D)	Zone 1/4	Zone 2/4	Zone 3/4	Zone 4/4
C1	1751.70	1365.90	1683.90	1628.60
D1	1514.13	1551.10	1486.5	1526.20
C2	2051.20	1654.90	1943.30	1956.90
D2	1659.90	1887.80	1822.80	1849.6
C3	2299.00	1940.00	2063.10	2215.40
D3	2025.30	2121.00	2095.10	2114.50
C4	2555.10	2154.20	1985.20	2290.00
D4	2247.00	2302.30	2326.90	2290.10
C5	2770.60	2330.20	2542.10	_
D5	2540.4	2471.60	2425.50	_
C6	3001.56	_	_	
D6	2793.50	_	_	
C7	3028.6	_	_	
D7	2996.1	_	_	

it should be noted the number of cycles concerning the pieces of bamboo taken from the stem in the area close to the base are higher than that of the pieces coming from the central parts and close to the foliage. The convincing explanation lies in the ability of the fibers constituting the samples of the base to have excellent mechanical properties.

The load slope data were used to plot the curves in **Figure 10**.

As we can see, the data in **Table 2** clearly show that the stiffness of material gradually increases as we pass from on cycle to the other. This highlights a plastification phenomenon which occurs within the material. In addition, the elastic modulus of the discharge slopes are all greater than those of the charge slopes. We can now investigate the state of degradation of the material via the calculation of the ratio between the respective slopes of the charge and discharge by means of the relation (3).

$$Y = \frac{E-}{E+} \tag{4}$$

In the literature, several research studies ([8] and [15]) agree that when the ratio is close to 1, this indicates the stability within the material. Conversely, as soon as this coefficient departs from 1, this implies degradation within material until it is completely broken (**Figure 10**).

By exploiting the different parameters, from **Table 2** and using them in relation 4, we plot the group of **Figure 10**.

Looking at the graph of **Figure 10**, it appears that at the charging start, the sample EP 2/4 G5 start with ratio 0.88. Then, from the third cycle until the fifth, the ratio gradually tends to 1. This would be an indicator of a slight deterioration within the material. However, it can be noted that 1/4 zone sample practically begins with the same ratio as that of the 2/4 zone and also tends towards 1 despite the number of high cycles. Conversely, the other samples drawn from the other two zones deviate significantly from 1 at the end of the cycles which sug-

gest that the samples taken away from the 1/4 zone near the base deteriorate fairly quickly when they are subjected to repeated cycles.

The analysis of the effect of the number of cycles on the residual strain is considered. Figure 11 shows the relationship between the numbers of cycles and residual strain.
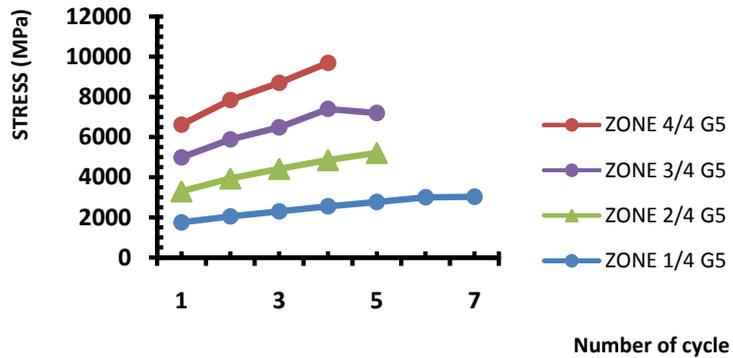

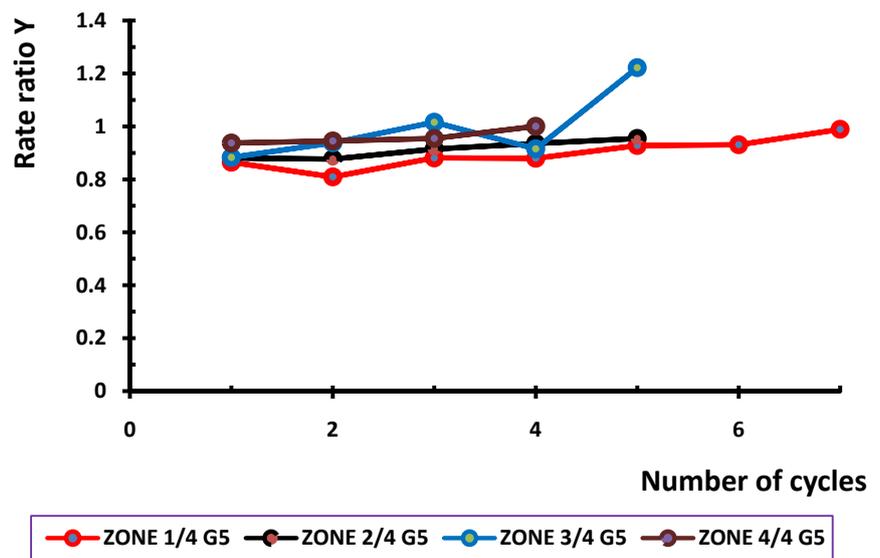**Figure 9.** Curves of the load modules as a function of the number of cycles.

Figure 10. Response curve rate charge-discharge according to the number of cycle.
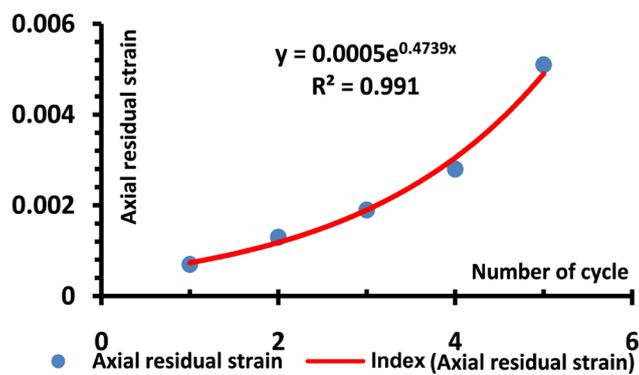

$y = 0.0005e^{0.4739x}$
$R^2 = 0.991$

Figure 11. Residual strain relation according to the number of cycle.

By taking account of the graph of Figure 11, it comes from the plastic deformation of increasing with the evolution of numbers of cycles and the stress. This ascent becomes very rapid from the third cycle to the fifth. The law of evolution between these two parameters is exponential.

4. Conclusions

Throughout this work, we have been investigating the effect of the cyclic charging bamboo compression. An experimental approach has been adopted. As a result, several results are established. Firstly, in the strain deformation area, the cyclic constrain generates the hysteresis formation loops. The area of these increases the number of cycles evolves, implying the increasing variation of the energy rate. Secondly, energy changes linearly as a function of number of cycles.

Indeed, on a bamboo rod, the samples taken from the area near the base store twice as much energy as those belonging to the top. Thirdly, the modulus of the charge and discharge curves change when the number of cycles increases.

Furthermore, the analysis of the ratio of the rigidities of the charge-discharge reveals that the samples from the base of the rod deteriorate less quickly than those taken from the top. Finally, an analysis based on the observation of the effect of the number of cycles on the residual strain shows an exponential law of evolution.

Conflicts of Interest

The authors declare no conflicts of interest regarding the publication of this paper.

References

[1] International Network for Bamboo and Rattan. http://www.inbar.int

[2] Sikame Tagne, N.R., Njeugna, E., Fogue, M., Drean, J.-Y., Nzeukou, A. and Fokwa, D. (2014) Study of Water Absorption in *Raffia vinifera* Fibres from Bandjoun, Cameroon. *The Scientific World Journal*, **2014**, Article ID: 912380. https://doi.org/10.1155/2014/912380

[3] Foadieng, E. (2012) Contribution à l'étude thermomécanique et viscoélastique du bambou de raphia. L. vinifera arecacea sous charges de flexion. Thèse de Doctorat Phd, Département des sciences physiques, Université de Dschang, Cameroun, non publié, 205 p.

[4] Foadieng, E., *et al.* (2017) Study of the Thermal Properties of Raffia Bamboo Vinifera L. Arecaceae. *Advances in Materials Sciences and Engineering*, **2017**, Article ID: 9868903. https://doi.org/10.1155/2017/9868903

[5] Janssen, J., *et al.* (1991) Bamboo as an Engineering Material. Bamboo and Rattan Research Network. International Development Research Centre, Singapore, No. 6, 100.

[6] Talla, P.K., Tekougnening, T., Tangka, J.R., Ebale, E. and Foudjet, A. (2004) Statistical Model of Strength in Compression of *Raphia vinifera* L. Arecacea. *Journal of Bamboo and Rattan*, **3**, 229-235. https://doi.org/10.1163/1569159041765290

[7] Adrawes, G.M. (2014) The Cyclic Loading of Normal Concrete in a Specific Stress

Range. *Jordan Journal of Civil Engineering*, **8**, 271-281.

[8] Breccolotti, M., Bonfigli, M.F., D'Alessandro, A. and Materazzi, A.L. (2015) Constitutive Modeling of Plain Concrete Subjected to Cyclic Uniaxial Compressive Loading. *Construction and Building Materials*, **94**, 172-180.
https://doi.org/10.1016/j.conbuildmat.2015.06.067

[9] Yang, X.L., Wang, H.L. and Zhao, Z.L. (2018) Cyclic Behavior of Confined Cement-Stabilized Rammed Earth Walls. *Shock and Vibration*, **2018**, Article ID: 2983052. https://doi.org/10.1155/2018/2983052

[10] Fozao, *et al.* (2014) An Extend Endochronic Theory Formulation of Plastically Deformed Damaged Indian Bamboo under Uniaxial Compression. *Journal of Applied and Computational Mathematics*, **3**, Article ID: 1000178.

[11] Pambou, N.C., Ikogou, S., Pitti, M. and Ekomy, A.S. (2015) Comportement mécanique de l'okoume (Aucoumea Klaineana Pierre) sous sollicitations cycliques en compression. 4e journée du GDR sciences du bois-Clermont Ferrand.

[12] Azeufack, U.G., *et al.* (2019) Mechanical Characterization and Measurement of the Damage of the *Pericopsis elata* (Assamela). *Word Journal of Engineering and Technology*, **7**, 256-269. https://doi.org/10.4236/wjet.2019.72017

[13] Fothe, T., *et al.* (2019) Damage Evaluation of Two Equatorial Hardwoods under Uniaxial Compression: Case of *Entandrophragma cylindricum* (Sapelli) and *Chlorophora exelcia* (Iroko). *World Journal of Engineering and Technology*, **7**, 549-558.
https://doi.org/10.4236/wjet.2019.74039

[14] International Standard ISO 22157 (2004) Bamboo—Determination of Physical and Mechanical Properties Part 1 (E).

[15] Guo, H.J., Ji, M., Zhang, Y.D. and Zhang, M. (2018) Study of Mechanical Property of Rock under Uniaxial Cyclic Loading and Unloading. *Advances in Civil Engineering*, **2018**, Article ID: 1670180. https://doi.org/10.1155/2018/1670180